

US ARMY  
MATERIEL  
COMMAND

AD-A170 361

12  
AD

## TECHNICAL REPORT BRL-TR-2741

# ELECTRICAL CONDUCTANCE OF LIQUID PROPELLANTS: THEORY AND RESULTS

John A. Vanderhoff  
Steven W. Bunte  
Philip M. Donmoyer

June 1986

DTIC  
ELECTE  
JUL 29 1986  
S D

FILE COPY

APPROVED FOR PUBLIC RELEASE; DISTRIBUTION UNLIMITED.

US ARMY BALLISTIC RESEARCH LABORATORY  
ABERDEEN PROVING GROUND, MARYLAND

86 7 29 043

Destroy this report when it is no longer needed.  
Do not return it to the originator.

Additional copies of this report may be obtained  
from the National Technical Information Service,  
U. S. Department of Commerce, Springfield, Virginia  
22161.

The findings in this report are not to be construed as an official  
Department of the Army position, unless so designated by other  
authorized documents.

The use of trade names or manufacturers' names in this report  
does not constitute indorsement of any commercial product.

UNCLASSIFIED

SECURITY CLASSIFICATION OF THIS PAGE (When Data Entered)

DD FORM 1473 EDITION OF 1 NOV 65 IS OBSOLETE  
, JAN 73

UNCLASSIFIED

SECURITY CLASSIFICATION OF THIS PAGE (When Data Entered)

## TABLE OF CONTENTS

	<u>Page</u>
LIST OF FIGURES.....	5
LIST OF TABLES.....	7
I. INTRODUCTION.....	9
II. EARLY WORK.....	9
III. IONIC INTERACTIONS.....	11
IV. ION-PAIRING.....	14
V. TEMPERATURE.....	15
VI. EXPERIMENT.....	16
VII. RESULTS AND DISCUSSION.....	16
VIII. SUMMARY.....	21
REFERENCES.....	27
DISTRIBUTION LIST.....	29

Accesion For	
NTIS CRA&I	<input checked="" type="checkbox"/>
DTIC TAB	<input type="checkbox"/>
Unannounced	<input type="checkbox"/>
Justification	.....
By _____	
Distribution /	
Availability Codes	
Dist	Avail and/or Special
A-1	

THIS DOCUMENT CONTAINED  
BLANK PAGES THAT HAVE  
BEEN DELETED



LIST OF FIGURES

<u>Figure</u>		<u>Page</u>
1	Picture of Ion Model for the Debye-Hückel Theory.....	12
2	Specific Conductance of HAN as a Function of Concentration in H <sub>2</sub> O at -12, 20, and 40°C.....	17
3	Equivalent Conductance of HAN as a Function of Concentration at -12, 20, and 40°C.....	18
4	Fit of Equivalent Conductance at 20°C With Wishaw-Stokes Equation, Data $\square$ , Fit --- Without Viscosity Correction, Fit — With Viscosity Correction.....	19
5	Equivalent Conductance of HAN as a Function of Concentration in H <sub>2</sub> O and in H <sub>2</sub> O-CH <sub>3</sub> OH Mixtures at 20 and 40°C.....	21
6	Specific Conductance of 11 M HAN, LGP 1845, and LGP 1846 as a Function of Temperature. Data are $\square$ , $\circ$ , $\Delta$ . Solid Lines are Polynomial Fits.....	22

LIST OF TABLES

<u>Table</u>	<u>Page</u>
1 Critical Distance for Monovalent Electrolyte Ion-Pairing at Various Temperatures and Dielectric Constants.....	15
2 Ionic Separations for Monovalent Electrolyte Solutions at Various Concentrations.....	15
3 The Specific and Equivalent Conductances of Aqueous HAN as a Function of Concentration for Three Temperatures; -12.2°C, 20.0°C, and 40.0°C.....	17
4 Viscosity of Water and Aqueous HAN as a Function of Concentration at 20°C.....	20
5 Specific Conductances of 11 M HAN as a Function of Temperature.....	23
6 Specific Conductance of LGP 1845 as a Function of Temperature.....	24
7 Specific Conductance of LGP 1846 as a Function of Temperature.....	25
8 Polynomial Coefficients Used for the Best Fit of the Temperature Dependent Conductance Data for 11 M HAN, LGP 1845, and LGP 1846.....	25

## I. INTRODUCTION

Candidate liquid gun propellants generally fall into the category of concentrated aqueous salt solutions. The most promising candidate contains hydroxylammonium nitrate (HAN) and triethanol ammonium nitrate (TEAN). In an effort to enlarge the data base for these solutions, measurements of the electrical conductance were performed. These measurements can be of great practical value in the design of electrically initiated liquid propellant combustion systems; moreover, the variation of the electrical conductance with parameters such as concentration, temperature, and solvent can provide information about the fundamental behavior of these materials. Definitions of electrical conductance and a simple, almost universal, a.c. circuit used in making conductivity measurements were introduced in a prior report.<sup>1</sup> The important parameters to be considered in producing a proper conductivity cell design were also discussed in detail. Some initial data on the conductance of aqueous HAN as a function of concentration were also presented.

This report contains data on the conductance-concentration dependence of aqueous HAN and the conductance-temperature dependence of aqueous HAN and two liquid gun propellants, LGP 1845 and LGP 1846. Both LGP 1845 and LGP 1846 consist of mixtures of aqueous HAN and TEAN. In addition, the report begins with a review of the historical development of the conductance theory of electrolytes. This review is included to aid the reader not familiar with the details of physical chemistry. Ion-pairing and conductance equations are developed in this review and are subsequently used in the interpretation of the data.

## II. EARLY WORK

An electrolyte is a solute, which upon dissolution into a solvent produces a solution which conducts current. Whether the electrolyte is considered as being strong or weak depends upon its degree of dissociation. Strong electrolytes are almost completely dissociated. In practice, conductance measurements involve very simple circuits. The properties of conductance have been studied for over 100 years. One of the early descriptions of electrical conductance came from the works of Arrhenius<sup>2</sup> and Ostwald.<sup>3</sup> The dissociation equilibrium is written as



where AB is the undissociated molecule, and  $K_c$  is the equilibrium constant. Application of the law of mass action yields

$$\frac{[A^+][B^-]}{[AB]} = K_c, \quad (2)$$

where the brackets denote the equilibrium concentrations of the enclosed species. It follows that

$$[A^+] = [B^-] = c \gamma \quad (3)$$

where  $c$  is the concentration of solute and  $\gamma$  is the fraction of ions free to carry current. Substitution of Eq. (3) into Eq. (2) results in the following expression

$$\frac{c^2 \gamma^2}{c(1-\gamma)} = K_c . \quad (4)$$

It was hypothesized that

$$\gamma = \frac{\Lambda}{\Lambda_0} , \quad (5)$$

where  $\Lambda$  is the equivalent conductance of the solution and  $\Lambda_0$  is the equivalent conductance at infinite dilution. Substitution of Eq. (5) into Eq. (4), with some rearranging of terms, produces the Ostwald dilution law for conductance;

$$\frac{1}{\Lambda} = \frac{1}{\Lambda_0} + \frac{c\Lambda}{K_c \Lambda_0^2} . \quad (6)$$

This expression explained the electrical conductance of weak electrolytes well, but was inadequate for describing the electrical conductance of strong electrolytes. The reason for this being that ionic crystals are made up completely of positive and negative ions arranged in a periodic lattice, hence no dissociation of neutral molecules takes place. However, experimental conductance data showed that the strong electrolytes produce some structure in solution which is non-conducting. From Eq. (6) a plot of  $1/\Lambda$  should be linear in concentration. This held true for some electrolytes, but certainly not all. During this time Kohlrausch<sup>4</sup> had developed a new technique for measuring the conductivity; the use of alternating current. He made many detailed measurements of the conductance of electrolytes, and obtained an empirical expression to describe the behavior of the conductance of dilute solutions as a function of concentration. This expression

$$\Lambda = \Lambda_0 - Dc^{1/2} \quad (7)$$

was called the Kohlrausch square root law and gives a different concentration dependence of the conductance than the Ostwald dilution law. At this point there was a dilemma. The prominence of Arrhenius and Ostwald made Eq. (6) the favored expression. To resolve this concentration dependence question, it took the development of an interionic attraction theory. Up to then, no consideration of the ions influencing each other was taken into account. Nonetheless, Eq. (6) described fairly well the behavior of dilute solutions of weak electrolytes in water and of strong electrolytes in solvents of low dielectric constant.

### III. IONIC INTERACTIONS

It was recognized that ionic interactions must be incorporated into the theory to describe the variation in conductivity with concentration. Considerable work was expended in an attempt to express the electrostatic potential as a sum over all pairs of ions, where each ion is considered as a discrete site of charge. This approach led to infinite sums and non-convergence. Instead of this method, Debye and Hückel<sup>5</sup> considered all of the ions, except a reference ion at the origin replaced by a continuous space charge whose density is a function of distance from the origin. The model as shown in Figure 1 is then a central ion of charge +e surrounded by an ion atmosphere of charge -e. This ion atmosphere may be envisioned as a charged spherical shell located at a distance  $a + 1/k_1$  from the center of the ion. The calculation is performed by combining Poisson's equation of electrostatic theory with Boltzmann's distribution law. The end result is an expression for the electric potential  $\psi$  of the form

$$\psi = \frac{Ae^{-k_1 r}}{r} , \quad (8)$$

where A and  $k_1$  are physical constants which are completely determined from the boundary conditions and known physical properties of the electrolyte. This work was a major breakthrough, and equations for various transport properties were derived shortly thereafter. A more complete mathematical discussion of the Debye and Hückel theory can be found in many texts; see for example Harned and Owen.<sup>6</sup> The theory of Debye and Hückel does have limits of application for several reasons. A point charge model is used which must necessarily fail at close range due to the finite size of the ions. In addition, this range is larger when considering asymmetrical ions. In the derivation of an analytic expression for the electric potential, an exponential is expanded and only two terms retained. The necessary condition for neglecting the rest of the series is that  $Ze\psi \ll kT$ , where Z, k, and T are the ion charge multiplicity, Boltzmann's constant, and the absolute temperature, respectively. Physically this means that the theory will break down more easily for multivalent ions, and values of  $\psi$  must be kept small by large separation of ions (dilute solutions).

The transport property of concern here is the electrical conductance,  $\Lambda$ . One of the first analytic expressions which used the electric potential of Debye and Hückel appeared in the work of Onsager.<sup>7</sup> Two main effects were considered in the interaction of the ions with an external field. First, an electrophoretic effect arises from the interaction of the spherical shell ion atmosphere with an external electric field. This field causes the shell and solvent molecules to move in one direction, while the central reference ion moves in the opposite direction, similar to swimming upstream. The other effect is the relaxation effect. When the external field is applied, the ions move and if the response were instantaneous then spherical symmetry would be preserved. However, frictional forces cause a time lag and an asymmetry arises. This asymmetry induces an internal field that opposes the external field and lowers the conductance. In light of these effects, Onsager developed the resultant expression

$$\Lambda = \Lambda_0 - (\alpha \Lambda_0 + \beta)c^{1/2} , \quad (9)$$

where  $\alpha$  and  $\beta$  are physical constants that are completely determined from the physical properties of the electrolyte. Here the  $\alpha \Lambda_0 c^{1/2}$  term arises from the relaxation effect, and the  $\beta c^{1/2}$  term is due to the electrophoretic effect. Onsager's equation is not strictly an equation for the conductance, but rather the equation for the tangent to the conductance curve in the limit of zero concentration. This result, and an earlier approximate result obtained by Debye and Hückel, showed that the equivalent conductance at low concentration is proportional to the square root of the concentration. These theoretical results were in exact agreement with the empirical square root law determined by Kohlrausch.

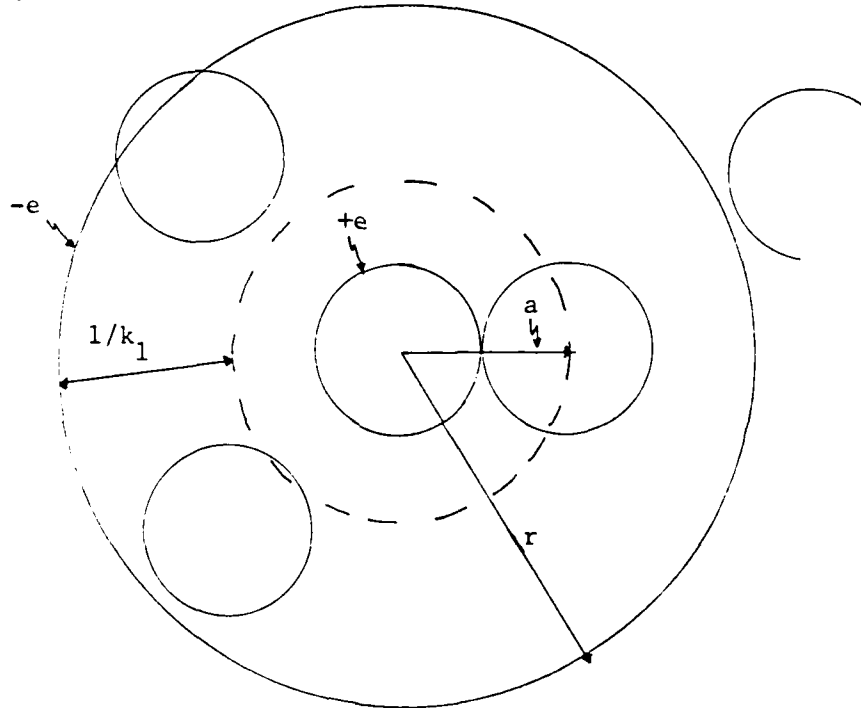


Figure 1. Picture of Ion Model for the Debye-Hückel Theory

A subsequent major step in the improvement of the equation for conductance at higher concentrations was attributed to Falkenhagen, et al.<sup>8</sup> They included the finite size of ions by not approximating the Debye-Hückel expression Eq. (8) for the electric potential. Here the physical constant  $\Lambda$  contains a term

$$\frac{k_1 a}{1+k_1 a} ,$$

which is only negligible at low concentrations. Falkenhagen, et al., retained this term in calculating the relaxation effect. The resulting expression for the conductance takes the form

$$\Lambda = [\Lambda_0 - \frac{\rho c^{1/2}}{1 + \tilde{B}ac^{1/2}}] \cdot [1 - \frac{\alpha c^{1/2} F}{1 + \tilde{B}ac^{1/2}}] \quad (10)$$

where  $\alpha$  and  $\beta$  are analogous to the constants of Onsager's limiting result. These parameters are conveniently expressed as

$$\alpha = \frac{8.20 \times 10^5}{(\epsilon T)^{3/2}}, \quad \beta = \frac{82.5}{n^0 (\epsilon T)^{1/2}}, \quad \text{and} \quad B = \frac{50.29}{(\epsilon T)^{1/2}}$$

where  $\epsilon$  and  $n^0$  are the dielectric constant and viscosity of the solvent, respectively. The distance  $a$  used here is in units of centimeters and  $\tilde{a} = a/10^{-8}$ . The term

$$F = \frac{\exp(-0.2929 k_1 a) - 1}{0.2929 k_1 a}$$

is more conveniently represented by

$$F = \frac{e^x - 1}{x} \quad \text{where} \quad x = 0.2929 \tilde{B}ac^{1/2}.$$

Equation (10) has a much larger applicable concentration range. However, at concentrations exceeding several molar, certain salt solutions show substantial deviations. It has been found that these deviations at high concentrations could be minimized by multiplying Eq. (10) by a relative fluidity factor  $(n^0/n)$ , where  $n$  is the viscosity of the solution. Equation (10) then becomes the well known Wishaw-Stokes<sup>9</sup> equation. Although this viscosity correction seems to work well, an assessment of the validity of this factor is complicated. A qualitative explanation of this correction is as follows. The bulk viscosity is the force required to move layers of solution with respect to each other. These shear forces are long range Coulomb forces and short range ion-water forces. As a general rule, strongly hydrated ions cause large increases in viscosity, while unhydrated ions do not. The Coulomb forces between ions have already been taken into account in the conductivity equation, thus it seems that only the short range forces have been neglected. Therefore, the viscosity should not be the bulk viscosity, but only a fraction of it. The justification for using the bulk viscosity is that the short range forces dominate in the concentrated region, and depend approximately linearly on the concentration.

The present state of the conductance theory for unassociated electrolytes is represented by Eqs. (9) and (10). The model from which these equations are derived fails at high concentration. However, no theory has been successful in the description of the conductance behavior of concentrated solutions. It has been suggested<sup>10</sup> that this description should properly start from a theory of fused salts, where the distribution function is a periodic and damped radial function. This function must approach the Debye-Hückel function in the limit of low concentration.

#### IV. ION-PAIRING

Up to this point, we have only discussed unassociated electrolytes; however, for the cases under consideration, namely nitrate salts, it is possible that ion pair formation occurs in regions of highest concentration.

For the present purpose, ion association is divided into two general classes. In the first class, the solid molecules do not completely dissociate into ions when dissolved. This is a property of weak electrolytes. In the second class, i.e., strong electrolytes, the solid phase ions exist in the form of a periodic lattice structure, and upon dissolution, become mobile. These ions in solution can then form some aggregate structure, where the net charge on the structure is zero, thus giving no contribution to the conductance. The simplest structure of this type is an ion-pair, which is the association that is of concern for the solutions studied here. There is a distinct difference in the non-conducting structures of these two classes: the undissociated molecule is a number of atoms held together by electronic bonds, whereas the ion-pair is held together entirely by electrostatic Coulomb forces, where neither the cation nor the anion lose their identity.

Early data clearly showed that some strong electrolytes must produce structures in solution which are non-conducting. In 1926, Bjerrum<sup>11</sup> proposed a criteria for the formation of ion-pairs, which essentially equates the thermal energy with the electrostatic energy of two oppositely charged ions. From this, a critical distance  $b$  can be obtained

$$b = \frac{|Z_1 Z_2| e^2}{2\epsilon kT} \quad (11)$$

where for distances equal to or smaller than  $b$ , the ions are considered paired. This is a simple approximation of conditions necessary for ion pairing. Nevertheless, it is instructive in showing the dependence of ion pairing on the various physical properties. It is obvious that multivalent ions have a greater tendency to ion pair. It is also evident from Eq. (11) that a decrease in the dielectric constant will increase ion-pair formation. Moreover it appears on the surface that decreasing the temperature increases ion-pairing, however, the dielectric constant is also temperature dependent to the point where increasing the temperature slightly favors ion pairing. For monovalent ions in water at room temperature, the critical distance  $b$  is 3.57 Å. It is of interest to calculate critical distances for monovalent ions as a function of temperature and dielectric constant, and then compare these critical distances with ionic separations which are predominantly a function of concentration. Tables 1 and 2 contain these comparisons. The dielectric constant was changed by using water and methanol as a solvent. Values for the ionic separation were obtained from an approximate empirical relationship for monovalent ions in solution,  $9.4 M^{-1/3}$  Å. Here  $M$  is the concentration in moles per liter. For methanol, it is seen that the critical radius is over twice as large as for solvent water. Moreover, the ionic separation values are such that one would expect some ion-pairing for methanol and not for water. Further discussion of ion-pairing in this context is given with the results for the conductance of HAN in water-methanol solvent mixtures.

Table 1. Critical Distance for Monovalent Electrolyte Ion-Pairing at Various Temperatures and Dielectric Constants

Temp. °C	Dielectric Constant, H <sub>2</sub> O	Critical Distance Solvent, H <sub>2</sub> O Å	Dielectric Const, CH <sub>3</sub> OH	Critical Distance Solvent, CH <sub>3</sub> OH Å
-50	--	--	49.5	7.7
-25	--	--	43.5	7.9
0	88	3.45	37.5	8.1
+25	78	3.57	32.0	8.7

Table 2. Ionic Separations for Monovalent Electrolyte Solutions at Various Concentrations

Concentration M	Ionic Separation 9.4M <sup>-1/3</sup> Å
6	5.17
9	4.52
11	4.23
13	4.00
15	3.81

## V. TEMPERATURE

Another important variable that deserves comment is the large temperature dependence of the conductance. There is nearly a five or six fold increase in the conductivity of a strong electrolyte when increasing the temperature from 0 to 100°C. This increase in conductance is due, at least in part, to the decrease in the viscosity of water. From Walden's Rule,  $\Lambda\eta = \text{const}$ , where  $\eta$  is the viscosity, it is observed that this product varies at most by 30% as a function of temperature. This suggests that viscous forces are responsible for most of the resistance to the motion of ions in water.

A majority of the conductance data have been reported at a temperature of 25°C, thus, Campbell, et al.,<sup>12</sup> have used the empirical relationship

$$\frac{\Lambda_t}{\Lambda_{25^\circ}} = 1 + a(t-25) + b(t-25)^2 + \dots \quad (13)$$

to fit the temperature dependence of the conductance for strong electrolytes. Here  $t$  is the temperature in °C and  $a$  and  $b$  are empirical constants. A form of Eq. (13) will be applied later to the temperature dependent data reported here.

## VI. EXPERIMENT

The measurement circuit and conductivity cell used to obtain the experimental data were very similar to that described in the first report.<sup>1</sup> The only difference is that the U-tube Pyrex cell was slightly shorter, giving a cell constant of 137.6 cm<sup>-1</sup>. The cell constant was checked with both sodium chloride and potassium chloride solutions. Current flowing through the solutions of interest was kept well below one milliampere. An audio frequency alternating current of 1 kHz was used for all of the data reported here, and all measurements were independent of frequency over the 500 Hz to 10 kHz range. For the temperature dependent studies, the U-tube conductivity cell was almost completely immersed in a Dewar filled with methanol or water. The temperature of conductivity cell was controlled manually with heating elements and cooling with dry ice or ice while being continuously stirred. The temperature was monitored with a digital readout platinum resistance thermometer, which gave temperatures to the nearest 0.1°F. The temperature control was  $\pm 0.1^{\circ}\text{F}$ .

Reagent or research grade chemicals and distilled water were used for this study. The preparation of 13 M HAN solutions, which were used as the starting point for the various aqueous HAN solutions, were prepared by concentrating high purity dilute solutions obtained from Southwest Analytical Chemicals, Inc., Austin, TX. The liquid gun propellants LGP 1845 and LGP 1846, are made of mixtures of HAN, TEAN and H<sub>2</sub>O. LGP 1845 contains (weight percent) 63.2% HAN, 20% TEAN, and 16.8% H<sub>2</sub>O. LGP 1846 contains (weight percent) 60.8% HAN, 19.2% TEAN, and 20% H<sub>2</sub>O.

## VII. RESULTS AND DISCUSSION

The specific conductance and equivalent conductance of HAN as a function of concentration in water for three temperatures, are shown on Figures 2 and 3, respectively. The data is tabulated in Table 3. Both the concentration and temperature dependence of the conductance is typical of monovalent salts dissolved in water. As shown in the first report,<sup>1</sup> the conductance of NaNO<sub>3</sub> as a function of concentration in water is very similar to that of HAN. It was observed that the specific conductance of HAN starts decreasing at concentrations greater than about 7 M at 20°C, whereas most other salts saturate in this concentration region. However, if these salt solutions are heated to increase the solubility limits, then the bending over phenomenon of the specific conductance is also observed. This decrease in the conductance as more ions are added suggests that the mobility of the ions is substantially diminished and/or the ions form non-conducting species. Most of the experimental data has been obtained at 20°C, so it is this data of Figure 3 that we will attempt to fit with Eq. (10), the Wishaw-Stokes equation. It should be noted that most of these concentrations severely push the limits of validity of this equation for concentration maximums; furthermore, not having an experimentally determined value for  $\Lambda_0$  causes questions at the very low concentrations.

SPECIFIC CONDUCTANCE OF HAN  
AT -12.2°C, 20.0°C, AND 40.0°C

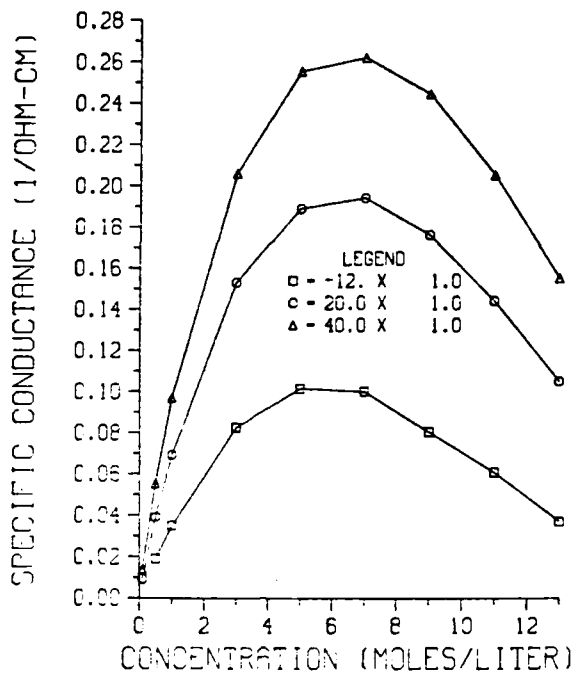


Figure 2. Specific Conductance of HAN as a Function of Concentration in  $\text{H}_2\text{O}$  at -12, 20, and 40°C

Table 3. The Specific and Equivalent Conductances of Aqueous HAN as a Function of Concentration for Three Temperatures; -12.2°C, 20.0°C, and 40.0°C

Concentration M	Sp. Cond.	Eq. Cond.	Sp. Cond.	Eq. Cond.	Sp. Cond.	Eq. Cond.
	$\Omega^{-1} \text{ cm}^{-1}$	$\text{cm}^2 \Omega^{-1}$	$\Omega^{-1} \text{ cm}^{-1}$	$\text{cm}^2 \Omega^{-1}$	$\Omega^{-1} \text{ cm}^{-1}$	$\text{cm}^2 \Omega^{-1}$
T = -12.2°C						
0.1	-----	----	.00924	92.4	.0140	140
0.5	.0191	38.3	.0390	78.1	.0555	111
1.0	.0350	35.0	.0693	69.3	.0970	97.0
3.0	.0825	27.5	.153	51.0	.206	68.6
5.0	.101	20.2	.189	37.8	.255	51.0
7.0	.0998	14.2	.194	27.7	.262	37.4
9.0	.0802	8.91	.176	19.6	.244	27.1
11.0	.0608	5.53	.144	13.1	.205	18.7
13.0	.0370	2.85	.105	8.08	.155	11.9

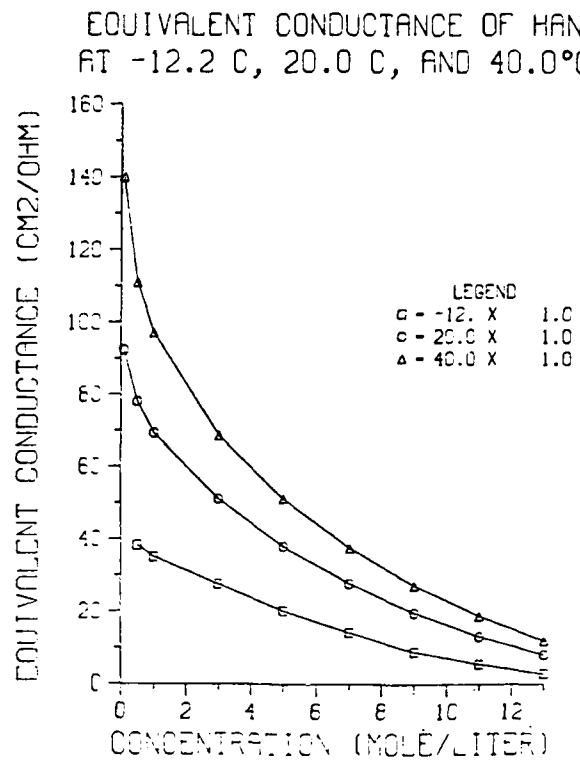


Figure 3. Equivalent Conductance of HAN as a Function of Concentration at -12, 20, and 40°C

Normally  $\Lambda_0$  is determined from an extrapolation of extremely low concentration data using a form of Eq. (7). In our experiments only one cell was used, which was tailored for accurate measurements of concentrated solutions. This design does not work well for dilute solutions; thus,  $\Lambda_0$  has been roughly estimated by analogy with other limiting conductances of salt solutions.  $\Lambda_0$  can be written as  $\Lambda_0 = \lambda_0^+ + \lambda_0^-$ , where  $\lambda_0^+$  and  $\lambda_0^-$  are the limiting equivalent conductances of the constituent cation and anion. For  $\text{NO}_3^-$ ,  $\lambda_0^-$  is 64 at 20°C, however, a value for  $\text{NH}_3\text{OH}^+$  has not been reported. We could say it is similar to  $\text{NH}_4^+$  which is 65, or choose an ion of similar molecular weight, say  $\text{CH}_3\text{NH}_3^+$ , which has a limiting equivalent conductance of about 53 at 20°C. From these considerations, a reasonable value for  $\Lambda_0$  for aqueous HAN solutions is  $64 + (59 \pm 6) = 123 \pm 6$  at 20°C.

For an aqueous monovalent electrolyte at 20°C, Eq. (10) becomes

$$\Lambda = [\Lambda_0 - \frac{53.48c^{1/2}}{1+0.3276\tilde{a}c^{1/2}}] [1 - \frac{0.2269c^{1/2}F}{1+0.3276\tilde{a}c^{1/2}}]$$

where  $c$  is expressed in moles per liter,  $\tilde{a}$  in angstroms and  $F = \frac{e^x - 1}{x}$  where  $x$  is equal to  $0.0959\tilde{a}c^{1/2}$ . With the data being  $\Lambda$  and  $c$ , a least squares analysis<sup>13</sup> of this equation was applied using  $\Lambda_0$  and  $\tilde{a}$  as adjustable parameters. The resulting fit is shown as a dashed line on Figure 4. The fit

is not good and the convergence values are physically unrealistic. Although  $\Lambda^{\circ}$  did not change appreciably from the estimated value, settling in at a value of 122, the best fit occurred with an  $a$  value of 0.87 Å. This value of the ion size parameter is too small since the estimated radius of the  $\text{NO}_3^-$  anion is 1.8 Å.

### FIT OF EQUIVALENT CONDUCTANCE $\Lambda^{\circ}$ TO THE WISHAW-STOKES EQUATION

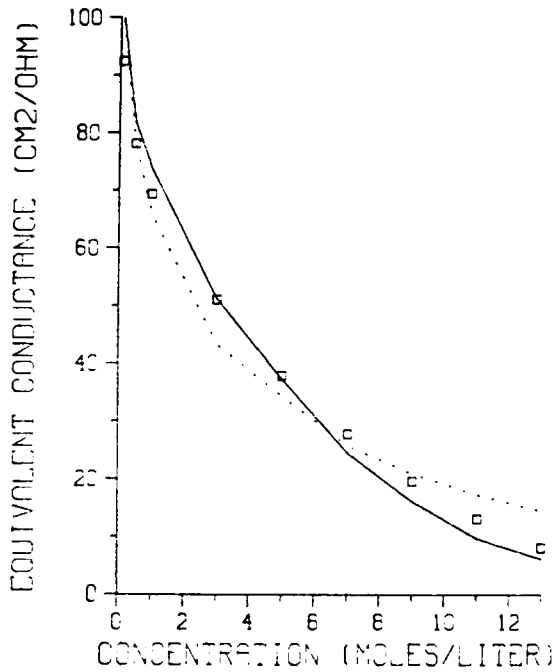


Figure 4. Fit of Equivalent Conductance at 20°C With Wishaw-Stokes Equation, Data  $\square$ , Fit --- Without Viscosity Correction, Fit — With Viscosity Correction

It was thought that a better fit might occur if we included a relative fluidity factor in the equation. However, there was no published data for the viscosity of aqueous HAN solutions, so a Brookfield viscometer was obtained and the viscosity of aqueous HAN measured as a function of concentration at 20°C. The results are tabulated in Table 4. With the inclusion of the relative fluidity factor, the least squares analysis gives the solid line shown on Figure 4. The best fit occurs with  $\Lambda^{\circ} = 112.3$  and  $\tilde{a} = 3.13$  Å. The  $a$  value is still a bit small, most monovalent aqueous salts fit to an  $a$  value between 4-5 Å, however it is much more realistic than before. The limiting equivalent conductance has changed by about 10% from our estimated value. This fit is better than the fit without the fluidity correction, but not great. Since Eq. (10) has been derived with approximations that are only valid for dilute solution conditions, and then a semi-empirical modification  $(\eta^{\circ}/\eta)$  applied to extend the concentration range, a precise fit is not to be expected.

Criteria for forming ion-pairs have been discussed earlier. From Tables 1 and 2 it is seen that under simple approximations, smaller dielectric constants favor ion-pairing. The numbers of Tables 1 and 2 suggest that ion-pairing is much more likely to occur in methanol than in water. To test this possibility, we measured the equivalent conductance of 13 M aqueous HAN mixed with various amounts of methanol. The concentration scale for the 13 M HAN-methanol mixtures is approximate since 13 M HAN was treated as pure HAN, this however, does not affect the qualitative behavior in which we are interested. The equivalent conductance of HAN in water and 13 M HAN in methanol as a function of concentration at 20 and 40°C is plotted in Figure 5. A significant difference is observed; for most of the concentration region the equivalent conductance for the methanol solvent is much lower. This behavior is also observed for  $\text{AgNO}_3$  solutions in solvents of different dielectric constant.<sup>14</sup> The smaller the dielectric constant, the more pronounced is the decrease in the conductance. From these results and also Raman spectra,<sup>14</sup> ion-pairs are presumed to be present in aqueous HAN-methanol solutions. We plan also to investigate the Raman spectra of HAN dissolved in different solvents. Thus far, the conductance results are qualitatively analogous to those found in  $\text{AgNO}_3$ . This indicates that ion-pairing is occurring when methanol is used as the solvent. Ion-pairing is probably minimal in aqueous HAN solutions.

Table 4. Viscosity of Water and Aqueous HAN as a Function of Concentration at 20°C. The Experimental Results are Obtained With a Brookfield Viscometer Calibrated With Distilled Water, and a Brookfield Standard Liquid of Known Viscosity

Species	Viscosity ( $\eta$ ) Centipoise	Viscosity Correction Factor $\eta^0/\eta$ , $\eta^0=1.002$
$\text{H}_2\text{O}$	1.002	1.00
0.1 M HAN	1.02	0.98
0.5 M	1.06	0.95
1.0 M	1.06	0.95
3.0 M	1.23	0.81
5.0 M	1.52	0.66
7.0 M	2.14	0.47
9.0 M	3.05	0.33
11.0 M	4.80	0.21
13.0 M	7.11	0.14

Finally the specific conductance of aqueous HAN and two candidate gun propellants, LGP 1845 and LGP 1846, has been measured as a function of temperature over the range from -60 to +60°C. The data are plotted in Figure 6 and tabulated in Tables 5, 6, and 7. Polynomial fits of this temperature data are also shown on Figure 6. Instead of applying the empirical relationship, Eq. (13), suited for 25°C conductance data, we chose a more general form which is

$$\Lambda = a_0 + a_1 t + a_2 t^2 + a_3 t^3$$

and applied a least squares analysis to the data. The resulting fits are quite good, and the best values of the coefficients are listed in Table 8. Again these three solutions studied have temperature dependences very similar to other common aqueous salt solutions.

### EQUIVALENT CONDUCTANCE OF HAN-H<sub>2</sub>O AND HAN-MeOH SOLUTIONS AT 20 AND 40 °C

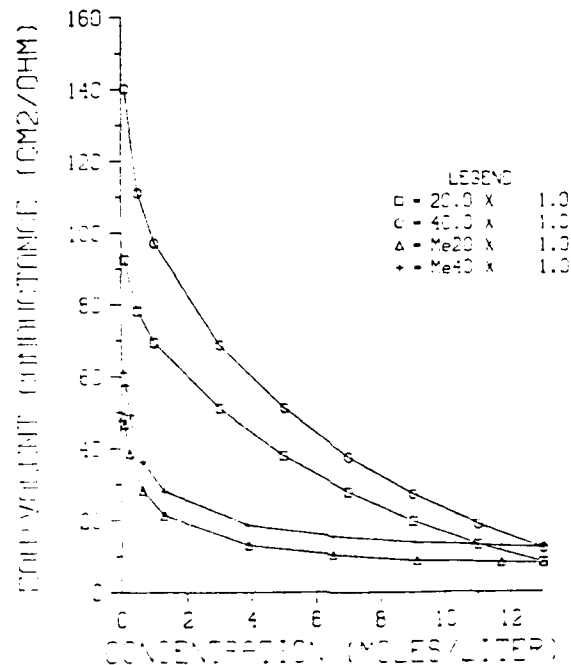


Figure 5. Equivalent Conductance of HAN as a Function of Concentration in H<sub>2</sub>O and in H<sub>2</sub>O-CH<sub>3</sub>OH Mixtures at 20 and 40°C

### VIII. SUMMARY

A brief historical review of the development of conductance theory has been reported and applied to the concentration dependent conductance data measured for aqueous HAN solutions. Specific conductance as a function of temperature for 11 M HAN, LGP 1845, and LGP 1846 has been measured and subsequently analyzed in terms of a polynomial equation. Two different solvents, water and methanol, have been used in the studies of HAN to assess the importance of ion-pairing. These data indicate that ion-pairing becomes more important with decreasing dielectric constant; a result consistent with the Bjerrum criteria and similar to previous results for other monovalent salts.

In general, the solutions studied here behave like most common monovalent salt solutions, with respect to the temperature and concentration dependence of the conductance. No evidence has been found for substantial ion-pairing for these aqueous salts, however, should these salts be dissolved in solvents of lower dielectric constant, ion-pairing will increase.

### SPECIFIC CONDUCTANCE OF 11M AND 1846

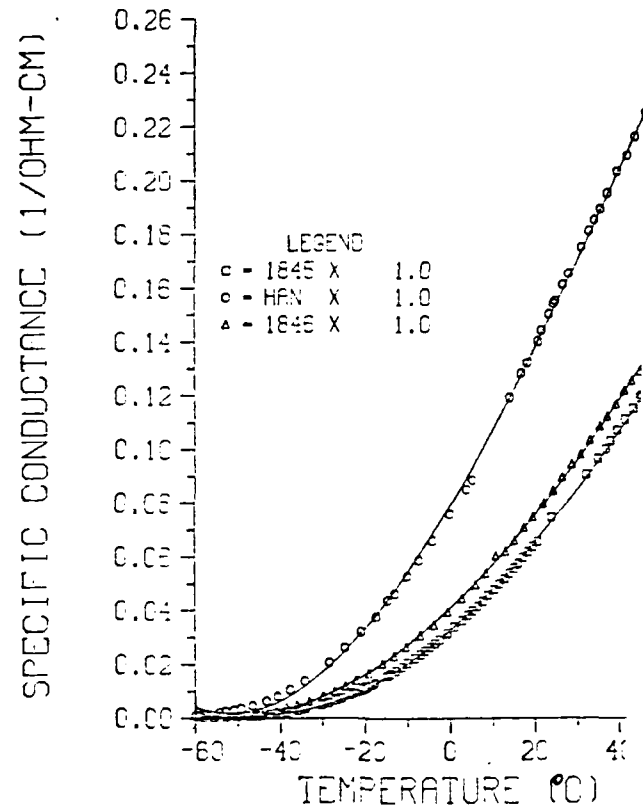


Figure 6. Specific Conductance of 11 M HAN, LGP 1845, and LGP 1846 as a Function of Temperature. Data are  $\square$ ,  $\circ$ ,  $\Delta$ . Solid Lines are Polynomial Fits

Table 5. Specific Conductance of 11 M HAN as a Function of Temperature

Temperature °C	Specific Conductance Ω <sup>-1</sup> cm
-59.9	9.00 x 10 <sup>-4</sup>
-59.0	1.03 x 10 <sup>-3</sup>
-57.9	1.26 x 10 <sup>-3</sup>
-54.4	1.91 x 10 <sup>-3</sup>
-52.9	2.41 x 10 <sup>-3</sup>
-51.0	2.91 x 10 <sup>-3</sup>
-49.2	3.36 x 10 <sup>-3</sup>
-46.6	4.51 x 10 <sup>-3</sup>
-43.3	6.27 x 10 <sup>-3</sup>
-40.7	8.07 x 10 <sup>-3</sup>
-37.7	1.05 x 10 <sup>-2</sup>
-34.2	1.38 x 10 <sup>-2</sup>
-28.4	2.07 x 10 <sup>-2</sup>
-24.7	2.62 x 10 <sup>-2</sup>
-20.9	3.21 x 10 <sup>-2</sup>
-17.3	3.77 x 10 <sup>-2</sup>
-14.6	4.38 x 10 <sup>-2</sup>
-13.0	4.62 x 10 <sup>-2</sup>
-10.0	5.26 x 10 <sup>-2</sup>
-7.3	5.86 x 10 <sup>-2</sup>
-4.1	6.58 x 10 <sup>-2</sup>
-0.6	7.56 x 10 <sup>-2</sup>
3.6	8.48 x 10 <sup>-2</sup>
4.9	8.83 x 10 <sup>-2</sup>
13.8	1.19 x 10 <sup>-1</sup>
16.6	1.28 x 10 <sup>-1</sup>
18.0	1.32 x 10 <sup>-1</sup>
20.6	1.40 x 10 <sup>-1</sup>
21.4	1.44 x 10 <sup>-1</sup>
23.2	1.50 x 10 <sup>-1</sup>
24.3	1.54 x 10 <sup>-1</sup>
24.7	1.55 x 10 <sup>-1</sup>
26.4	1.61 x 10 <sup>-1</sup>
27.8	1.65 x 10 <sup>-1</sup>
30.7	1.75 x 10 <sup>-1</sup>
32.5	1.81 x 10 <sup>-1</sup>
33.8	1.85 x 10 <sup>-1</sup>
35.2	1.89 x 10 <sup>-1</sup>
36.9	1.95 x 10 <sup>-1</sup>
39.2	2.03 x 10 <sup>-1</sup>
41.6	2.09 x 10 <sup>-1</sup>
43.5	2.16 x 10 <sup>-1</sup>
46.0	2.25 x 10 <sup>-1</sup>
49.0	2.35 x 10 <sup>-1</sup>
53.0	2.48 x 10 <sup>-1</sup>
53.8	2.50 x 10 <sup>-1</sup>

Table 6. Specific Conductance of LGP 1845 as a Function of Temperature

Temperature °C	Specific Conductance $\Omega^{-1} \text{ cm}^{-1}$	Temperature °C	Specific Conductance $\Omega^{-1} \text{ cm}^{-1}$
-47.0	$8.20 \times 10^{-4}$	5.2	$3.98 \times 10^{-2}$
-44.9	$9.54 \times 10^{-4}$	6.3	$4.15 \times 10^{-2}$
-42.5	$1.42 \times 10^{-3}$	7.6	$4.33 \times 10^{-2}$
-40.9	$1.73 \times 10^{-3}$	8.8	$4.56 \times 10^{-2}$
-38.6	$2.16 \times 10^{-3}$	10.2	$4.77 \times 10^{-2}$
-35.9	$2.98 \times 10^{-3}$	11.5	$4.98 \times 10^{-2}$
-34.2	$3.53 \times 10^{-3}$	12.7	$5.17 \times 10^{-2}$
-30.3	$5.03 \times 10^{-3}$	13.8	$5.37 \times 10^{-2}$
-28.7	$5.76 \times 10^{-3}$	14.9	$5.57 \times 10^{-2}$
-26.9	$6.67 \times 10^{-3}$	15.9	$5.75 \times 10^{-2}$
-25.5	$7.41 \times 10^{-3}$	17.1	$5.96 \times 10^{-2}$
-23.7	$8.69 \times 10^{-3}$	18.3	$6.16 \times 10^{-2}$
-22.8	$9.29 \times 10^{-3}$	19.4	$6.37 \times 10^{-2}$
-21.8	$9.97 \times 10^{-3}$	20.5	$6.55 \times 10^{-2}$
-21.2	$1.04 \times 10^{-2}$	23.9	$7.46 \times 10^{-2}$
-20.7	$1.08 \times 10^{-2}$	31.8	$9.06 \times 10^{-2}$
-20.1	$1.13 \times 10^{-2}$	34.6	$9.63 \times 10^{-2}$
-19.5	$1.17 \times 10^{-2}$	36.5	$1.00 \times 10^{-1}$
-18.6	$1.24 \times 10^{-2}$	37.6	$1.03 \times 10^{-1}$
-17.8	$1.31 \times 10^{-2}$	39.2	$1.07 \times 10^{-1}$
-14.8	$1.57 \times 10^{-2}$	41.0	$1.11 \times 10^{-1}$
-14.0	$1.64 \times 10^{-2}$	43.0	$1.15 \times 10^{-1}$
-12.8	$1.77 \times 10^{-2}$	44.6	$1.19 \times 10^{-1}$
-11.4	$1.90 \times 10^{-2}$	45.0	$1.20 \times 10^{-1}$
-10.0	$2.06 \times 10^{-2}$	46.2	$1.22 \times 10^{-1}$
-8.3	$2.23 \times 10^{-2}$	47.9	$1.26 \times 10^{-1}$
-7.0	$2.38 \times 10^{-2}$	49.7	$1.30 \times 10^{-1}$
-5.9	$2.50 \times 10^{-2}$	51.8	$1.35 \times 10^{-1}$
-4.7	$2.64 \times 10^{-2}$	54.3	$1.41 \times 10^{-1}$
-3.7	$2.77 \times 10^{-2}$	55.6	$1.44 \times 10^{-1}$
-2.5	$2.91 \times 10^{-2}$	56.8	$1.47 \times 10^{-1}$
-0.8	$3.14 \times 10^{-2}$	59.4	$1.53 \times 10^{-1}$
0.9	$3.40 \times 10^{-2}$		
2.7	$3.62 \times 10^{-2}$		
4.1	$3.82 \times 10^{-2}$		

Table 7. Specific Conductance of LGP 1846 as a Function of Temperature

Temperature °C	Specific Conductance $\Omega^{-1} \text{ cm}^{-1}$	Temperature °C	Specific Conductance $\Omega^{-1} \text{ cm}^{-1}$
-60.1	$1.96 \times 10^{-4}$	2.7	$4.45 \times 10^{-2}$
-57.9	$2.72 \times 10^{-4}$	5.9	$4.95 \times 10^{-2}$
-55.6	$3.52 \times 10^{-4}$	8.3	$5.37 \times 10^{-2}$
-52.9	$5.27 \times 10^{-4}$	10.7	$6.03 \times 10^{-2}$
-50.2	$8.30 \times 10^{-4}$	12.9	$6.19 \times 10^{-2}$
-47.7	$1.17 \times 10^{-3}$	15.1	$6.59 \times 10^{-2}$
-44.5	$1.81 \times 10^{-3}$	17.4	$7.07 \times 10^{-2}$
-41.1	$2.67 \times 10^{-3}$	19.5	$7.47 \times 10^{-2}$
-38.6	$4.22 \times 10^{-3}$	21.8	$7.97 \times 10^{-2}$
-36.1	$5.14 \times 10^{-3}$	24.1	$8.44 \times 10^{-2}$
-33.2	$6.32 \times 10^{-3}$	26.2	$8.94 \times 10^{-2}$
-29.9	$8.19 \times 10^{-3}$	28.4	$9.41 \times 10^{-2}$
-27.2	$9.94 \times 10^{-3}$	30.6	$9.79 \times 10^{-2}$
-24.7	$1.18 \times 10^{-2}$	32.8	$1.03 \times 10^{-1}$
-22.1	$1.40 \times 10^{-2}$	35.2	$1.08 \times 10^{-1}$
-19.1	$1.67 \times 10^{-2}$	36.9	$1.12 \times 10^{-1}$
-15.8	$2.03 \times 10^{-2}$	39.0	$1.17 \times 10^{-1}$
-13.1	$2.31 \times 10^{-2}$	40.9	$1.22 \times 10^{-1}$
-10.3	$2.64 \times 10^{-2}$	42.6	$1.25 \times 10^{-1}$
-7.0	$3.08 \times 10^{-2}$	44.5	$1.29 \times 10^{-1}$
-3.8	$3.45 \times 10^{-2}$	46.7	$1.36 \times 10^{-1}$
-0.6	$3.94 \times 10^{-2}$	48.9	$1.40 \times 10^{-1}$
		51.1	$1.46 \times 10^{-1}$
		53.4	$1.51 \times 10^{-1}$
		55.6	$1.57 \times 10^{-1}$
		57.8	$1.65 \times 10^{-1}$
		60.0	$1.71 \times 10^{-1}$
		62.2	$1.77 \times 10^{-1}$

Table 8. Polynomial Coefficients Used for the Best Fit of the Temperature Dependent Conductance Data for 11 M HAN, LGP 1845, and LGP 1846

Species	$\Omega^{-1} \text{ cm}^{-1} \text{ }^{\circ}\text{C}^{-1}$	$\Omega^{-1} \text{ cm}^{-1} \text{ }^{\circ}\text{C}^{-2}$	$\Omega^{-1} \text{ cm}^{-1} \text{ }^{\circ}\text{C}^{-3}$
11 M HAN	$3.282 \times 10^{-2}$	$1.385 \times 10^{-3}$	$1.362 \times 10^{-5}$
LGP 1845	$7.915 \times 10^{-2}$	$2.670 \times 10^{-3}$	$1.651 \times 10^{-5}$
LGP 1846	$4.099 \times 10^{-2}$	$1.495 \times 10^{-3}$	$1.244 \times 10^{-5}$

## REFERENCES

1. J.A. Vanderhoff and S.W. Bunte, "Conductance Measurements of Hydroxylammonium Nitrate," BRL Memorandum Report, in press.
2. S. Arrhenius, "Über die Dissociation der in Wasser gelösten Stoffe," Z. Physik. Chem., Vol. 1, p. 631, 1887.
3. W. Ostwald, "Über die Dissociations theorie der Elektrolyte," Z. Physik, Chem., Vol. 2, p. 270, 1888.
4. F. Kohlrausch and L. Holborn, "Das Leitvermögen der Elektrolyte," Teubner, Leipzig, 1916.
5. P. Debye and E. Hückel, "The Theory of Electrolytes. I. Lowering of Freezing Point and Related Phenomena," Physik. Z., Vol. 24, p. 185, 1923.
6. H.S. Harned and B.B. Owen, The Physical Chemistry of Electrolytic Solutions, 3rd Ed., Reinhold Publishing Corp., New York, NY, 1958.
7. L. Onsager, "The Theory of Electrolytes. II.," Physik. Z., Vol. 28, p. 277, 1927.
8. H. Falkenhagen, M. Leist, and G. Kelbg, "Theory of the Conductivity of Strong, Nonassociative Electrolytes at Higher Concentrations," Annals Physik, Vol. 6(II), p. 51, 1952.
9. B.F. Wishaw and R.H. Stokes, "The Diffusion Coefficients and Conductances of Some Concentrated Electrolyte Solutions at 25°C," J. Am. Chem. Soc., Vol. 76, p. 2065, 1954.
10. R.M. Fuoss and F. Accascina, Electrolytic Conductance, Interscience Publishers, Inc., New York, NY, 1959.
11. N.K. Bjerrum, Danske Vidensk. Selsk., Vol. 7, 1926, No. 9, "Selected Papers," p. 108, Einar Munksgaard, Copenhagen, 1949.
12. A.N. Campbell, A.P. Gray, and E.M. Kartzmark, "Conductances, Densities, and Fluidities of Solutions of Silver Nitrate and Ammonium Nitrate at 35°C," Can. J. Chem., Vol. 31, p. 617, 1953.
13. W.E. Wentworth, "Rigorous Least Squares Adjustment: Application to Some Non-Linear Equations, 1," J. Chem. Ed., Vol. 42, No. 2, p. 96, 1965.
14. G.J. Janz, "Studies of Ionic Association and Solution with Raman Laser Spectroscopy," Electroanalytical Chemistry and Interfacial Electrochemistry, Vol. 29, p. 107, 1971.

DISTRIBUTION LIST

<u>No. Of Copies</u>	<u>Organization</u>	<u>No. Of Copies</u>	<u>Organization</u>
12	Administrator Defense Technical Info Center ATTN: DTIC-DDA Cameron Station Alexandria, VA 22304-6145	1	Commander US Army Aviation Research and Development Command ATTN: AMSAV-E 4300 Goodfellow Blvd. St. Louis, MO 63120
1	HQ DA DAMA-ART-M Washington, DC 20310	1	Director US Army Air Mobility Research and Development Laboratory Ames Research Center Moffett Field, CA 94035
1	Commander US Army Materiel Command ATTN: AMCDRA-ST 5001 Eisenhower Avenue Alexandria, VA 22333-0001	4	Commander US Army Research Office ATTN: R. Ghirardelli D. Mann R. Singleton R. Shaw P.O. Box 12211 Research Triangle Park, NC 27709-2211
10	Central Intelligence Agency Office of Central Reference Dissemination Branch Room GE-47 HQS Washington, DC 20505		
1	Commander Armament R&D Center US Army AMCCOM ATTN: SMCAR-TSS Dover, NJ 07801	1	Commander US Army Communications - Electronics Command ATTN: AMSEL-ED Fort Monmouth, NJ 07703
1	Commander Armament R&D Center US Army AMCCOM ATTN: SMCAR-TDC Dover, NJ 07801	1	Commander ERADCOM Technical Library ATTN: DELSD-L, Reports Section Fort Monmouth, NJ 07703-5301
1	Director Benet Weapons Laboratory Armament R&D Center US Army AMCCOM ATTN: SMCAR-LCB-TL Watervliet, NY 12189	2	Commander Armament R&D Center US Army AMCCOM ATTN: SMCAR-LCA-G, D.S. Downs J.A. Lannon Dover, NJ 07801
1	Commander US Army Armament, Munitions and Chemical Command ATTN: SMCAR-ESP-L Rock Island, IL 61299	1	Commander Armament R&D Center US Army AMCCOM ATTN: SMCAR-LC-G, L. Harris Dover, NJ 07801

DISTRIBUTION LIST

<u>No. Of Copies</u>	<u>Organization</u>	<u>No. Of Copies</u>	<u>Organization</u>
1	Commander Armament R&D Center US Army AMCCOM ATTN: SMCAR-SCA-T, L. Stiefel Dover, NJ 07801	1	Commander US Army Development and Employment Agency ATTN: MODE-TED-SAB Fort Lewis, WA 98433
1	Commander US Army Missile Command Research, Development and Engineering Center ATTN: AMSMI-RD Redstone Arsenal, AL 35898	1	Office of Naval Research Department of the Navy ATTN: R.S. Miller, Code 432 800 N. Quincy Street Arlington, VA 22217
1	Commander US Army Missile and Space Intelligence Center ATTN: AMSMI-YDL Redstone Arsenal, AL 35898-5000	1	Commander Naval Air Systems Command ATTN: J. Ramnarace, AIR-54111C Washington, DC 20360
2	Commander US Army Missile Command ATTN: AMSMI-RK, D.J. Ifshin W. Wharton Redstone Arsenal, AL 35898	2	Commander Naval Ordnance Station ATTN: C. Irish P.L. Stang, Code 515 Indian Head, MD 20640
1	Commander US Army Missile Command ATTN: AMSMI-RKA, A.R. Maykut Redstone Arsenal, AL 35898-5249	1	Commander Naval Surface Weapons Center ATTN: J.L. East, Jr., G-23 Dahlgren, VA 22448-5000
1	Commander US Army Tank Automotive Command ATTN: AMSTA-TSL Warren, MI 48397-5000	1	Commander Naval Surface Weapons Center ATTN: R. Bernecker, R-13 G.B. Wilmot, R-16 Silver Spring, MD 20902-5000
1	Director US Army TRADOC Systems Analysis Activity ATTN: ATAA-SL White Sands Missile Range, NM 88002	2	Commander Naval Weapons Center ATTN: R.L. Derr, Code 389 China Lake, CA 93555
1	Commandant US Army Infantry School ATTN: ATSH-CD-CSO-OR Fort Benning, GA 31905		Commander Naval Weapons Center ATTN: Code 3891, T. Boggs K.J. Graham China Lake, CA 93555

DISTRIBUTION LIST

<u>No. Of Copies</u>	<u>Organization</u>	<u>No. Of Copies</u>	<u>Organization</u>
5	Commander Naval Research Laboratory ATTN: M.C. Lin J. McDonald E. Oran J. Shnur R.J. Doyle, Code 6110 Washington, DC 20375	4	National Bureau of Standards ATTN: J. Hastie M. Jacox T. Kashiwagi H. Semerjian US Department of Commerce Washington, DC 20234
1	Commanding Officer Naval Underwater Systems Center Weapons Dept. ATTN: R.S. Lazar/Code 36301 Newport, RI 02840	1	OSD/SDIO/UST ATTN: L.H. Caveny Pentagon Washington, DC 20301-7100
1	Superintendent Naval Postgraduate School Dept. of Aeronautics ATTN: D.W. Netzer Monterey, CA 93940	1	Aerojet Solid Propulsion Co. ATTN: P. Micheli Sacramento, CA 95813
4	AFRPL/DY, Stop 24 ATTN: R. Corley R. Geisler J. Levine D. Weaver Edwards AFB, CA 93523-5000	1	Applied Combustion Technology, Inc. ATTN: A.M. Varney P.O. Box 17885 Orlando, FL 32860
1	AFRPL/MKPB, Stop 24 ATTN: B. Goshgarian Edwards AFB, CA 93523-5000	2	Applied Mechanics Reviews The American Society of Mechanical Engineers ATTN: R.E. White A.B. Wenzel 345 E. 47th Street New York, NY 10017
1	AFOSR ATTN: J.M. Tishkoff Bolling Air Force Base Washington, DC 20332	1	Atlantic Research Corp. ATTN: M.K. King 5390 Cherokee Avenue Alexandria, VA 22314
1	Air Force Armament Laboratory ATTN: AFATL/DLODL Eglin AFB, FL 32542-5000	1	Atlantic Research Corp. ATTN: R.H.W. Waesche 7511 Wellington Road Gainesville, VA 22065
1	NASA Langley Research Center Langley Station ATTN: G.B. Northam/MS 168 Hampton, VA 23365	1	AVCO Everett Rsch. Lab. Div. ATTN: D. Stickler 2385 Revere Beach Parkway Everett, MA 02149

DISTRIBUTION LIST

<u>No. Of Copies</u>	<u>Organization</u>	<u>No. Of Copies</u>	<u>Organization</u>
1	Battelle Memorial Institute Tactical Technology Center ATTN: J. Huggins 505 King Avenue Columbus, OH 43201	2	General Motors Rsch Labs Physics Department ATTN: T. Sloan R. Teets Warren, MI 48090
1	Cohen Professional Services ATTN: N.S. Cohen 141 Channing Street Redlands, CA 92373	2	Hercules, Inc. Allegany Ballistics Lab. ATTN: R.R. Miller E.A. Yount P.O. Box 210 Cumberland, MD 21501
1	Exxon Research & Eng. Co. Government Research Lab ATTN: A. Dean P.O. Box 48 Linden, NJ 07036	1	Hercules, Inc. Bacchus Works ATTN: K.P. McCarty P.O. Box 98 Magna, UT 84044
1	Ford Aerospace and Communications Corp. DIVAD Division Div. Hq., Irvine ATTN: D. Williams Main Street & Ford Road Newport Beach, CA 92663	1	Honeywell, Inc. Government and Aerospace Products ATTN: D.E. Broden/ MS MN50-2000 600 2nd Street NE Hopkins, MN 55343
1	General Applied Science Laboratories, Inc. ATTN: J.I. Erdos 425 Merrick Avenue Westbury, NY 11590	1	IBM Corporation ATTN: A.C. Tam Research Division 5600 Cottle Road San Jose, CA 95193
1	General Electric Armament & Electrical Systems ATTN: M.J. Bulman Lakeside Avenue Burlington, VT 05401	1	IIT Research Institute ATTN: R.F. Remaly 10 West 35th Street Chicago, IL 60616
1	General Electric Company 2352 Jade Lane Schenectady, NY 12309	2	Director Lawrence Livermore National Laboratory ATTN: C. Westbrook M. Costantino P.O. Box 808 Livermore, CA 94550
1	General Electric Ordnance Systems ATTN: J. Mandzy 100 Plastics Avenue Pittsfield, MA 01203		

DISTRIBUTION LIST

<u>No. Of Copies</u>	<u>Organization</u>	<u>No. Of Copies</u>	<u>Organization</u>
1	Lockheed Missiles & Space Co. ATTN: George Lo 3251 Hanover Street Dept. 52-35/B204/2 Palo Alto, CA 94304	4	Sandia National Laboratories Combustion Sciences Dept. ATTN: R. Cattolica S. Johnston P. Mattern D. Stephenson Livermore, CA 94550
1	Los Alamos National Lab ATTN: B. Nichols T7, MS-B284 P.O. Box 1663 Los Alamos, NM 87545	1	Science Applications, Inc. ATTN: R.B. Edelman 23146 Cumorah Crest Woodland Hills, CA 91364
1	National Science Foundation ATTN: A.B. Harvey Washington, DC 20550	1	Science Applications, Inc. ATTN: H.S. Pergament 1100 State Road, Bldg. N Princeton, NJ 08540
1	Olin Corporation Smokeless Powder Operations ATTN: V. McDonald P.O. Box 222 St. Marks, FL 32355	3	SRI International ATTN: G. Smith D. Crosley D. Golden 333 Ravenswood Avenue Menlo Park, CA 94025
1	Paul Gough Associates, Inc. ATTN: P.S. Gough 1048 South Street Portsmouth, NH 03801	1	Stevens Institute of Tech. Davidson Laboratory ATTN: R. McAlevy, III Hoboken, NJ 07030
2	Princeton Combustion Research Laboratories, Inc. ATTN: M. Summerfield N.A. Messina 475 US Highway One Monmouth Junction, NJ 08852	1	Textron, Inc. Bell Aerospace Co. Division ATTN: T.M. Ferger P.O. Box 1 Buffalo, NY 14240
1	Hughes Aircraft Company ATTN: T.E. Ward 8433 Fallbrook Avenue Canoga Park, CA 91303	1	Thiokol Corporation Elkton Division ATTN: W.N. Brundige P.O. Box 241 Elkton, MD 21921
1	Rockwell International Corp. Rocketdyne Division ATTN: J.E. Flanagan/HB02 6633 Canoga Avenue Canoga Park, CA 91304	1	Thiokol Corporation Huntsville Division ATTN: R. Glick Huntsville, AL 35807

DISTRIBUTION LIST

<u>No. Of Copies</u>	<u>Organization</u>	<u>No. Of Copies</u>	<u>Organization</u>
3	Thiokol Corporation Wasatch Division ATTN: S.J. Bennett P.O. Box 524 Brigham City, UT 84302	1	California Institute of Tech. Jet Propulsion Laboratory ATTN: MS 125/159 4800 Oak Grove Drive Pasadena, CA 91103
1	TRW ATTN: M.S. Chou MSR1-1016 1 Parke Redondo Beach, CA 90278	1	California Institute of Technology ATTN: F.E.C. Culick/ MC 301-46 204 Karman Lab. Pasadena, CA 91125
1	United Technologies ATTN: A.C. Eckbreth East Hartford, CT 06108	1	University of California, Berkeley Mechanical Engineering Dept. ATTN: J. Daily Berkeley, CA 94720
3	United Technologies Corp. Chemical Systems Division ATTN: R.S. Brown T.D. Myers (2 copies) P.O. Box 50015 San Jose, CA 95150-0015	1	University of California Los Alamos Scientific Lab. P.O. Box 1663, Mail Stop B216 Los Alamos, NM 87545
2	United Technologies Corp. ATTN: R.S. Brown R.O. McLaren P.O. Box 358 Sunnyvale, CA 94086	2	University of California, Santa Barbara Quantum Institute ATTN: K. Schofield M. Steinberg Santa Barbara, CA 93106
1	Universal Propulsion Company ATTN: H.J. McSpadden Black Canyon Stage 1 Box 1140 Phoenix, AZ 85029	2	University of Southern California Dept. of Chemistry ATTN: S. Benson C. Wittig Los Angeles, CA 90007
1	Veritay Technology, Inc. ATTN: E.B. Fisher 4845 Millersport Highway P.O. Box 305 East Amherst, NY 14051-0305	1	Case Western Reserve Univ. Div. of Aerospace Sciences ATTN: J. Tien Cleveland, OH 44135
1	Brigham Young University Dept. of Chemical Engineering ATTN: M.W. Beckstead Provo, UT 84601	1	Cornell University Department of Chemistry ATTN: T.A. Cool Baker Laboratory Ithaca, NY 14853

DISTRIBUTION LIST

<u>No. Of Copies</u>	<u>Organization</u>	<u>No. Of Copies</u>	<u>Organization</u>
1	Univ. of Dayton Rsch Inst. ATTN: D. Campbell AFRPL/PAP Stop 24 Edwards AFB, CA 93523	3	Pennsylvania State University Applied Research Laboratory ATTN: K.K. Kuo H. Palmer M. Micci University Park, PA 16802
1	University of Florida Dept. of Chemistry ATTN: J. Winefordner Gainesville, FL 32611	1	Polytechnic Institute of NY Graduate Center ATTN: S. Lederman Route 110 Farmingdale, NY 11735
3	Georgia Institute of Technology School of Aerospace Engineering ATTN: E. Price W.C. Strahle B.T. Zinn Atlanta, GA 30332	2	Princeton University Forrestal Campus Library ATTN: K. Brezinsky I. Glassman P.O. Box 710 Princeton, NJ 08540
1	University of Illinois Dept. of Mech. Eng. ATTN: H. Krier 144MEB, 1206 W. Green St. Urbana, IL 61801	1	Princeton University MAE Dept. ATTN: F.A. Williams Princeton, NJ 08544
1	Johns Hopkins University/APL Chemical Propulsion Information Agency ATTN: T.W. Christian Johns Hopkins Road Laurel, MD 20707	1	Purdue University School of Aeronautics and Astronautics ATTN: J.R. Osborn Grissom Hall West Lafayette, IN 47906
1	University of Michigan Gas Dynamics Lab Aerospace Engineering Bldg. ATTN: G.M. Faeth Ann Arbor, MI 48109-2140	1	Purdue University Department of Chemistry ATTN: E. Grant West Lafayette, IN 47906
1	University of Minnesota Dept. of Mechanical Engineering ATTN: E. Fletcher Minneapolis, MN 55455	2	Purdue University School of Mechanical Engineering ATTN: N.M. Laurendeau S.N.B. Murthy TSPC Chaffee Hall West Lafayette, IN 47906
1	Rensselaer Polytechnic Inst. Dept. of Chemical Engineering ATTN: A. Fontijn Troy, NY 12181		

DISTRIBUTION LIST

<u>No. Of</u>	<u>Copies</u>	<u>Organization</u>
1		Stanford University Dept. of Mechanical Engineering ATTN: R. Hanson Stanford, CA 94305
1		University of Texas Dept. of Chemistry ATTN: W. Gardiner Austin, TX 78712
1		University of Utah Dept. of Chemical Engineering ATTN: G. Flandro Salt Lake City, UT 84112
1		Virginia Polytechnic Institute and State University ATTN: J.A. Schetz Blacksburg, VA 24061
1		Commandant USAFAS ATTN: ATSF-TSM-CN Fort Sill, OK 73503-5600

Aberdeen Proving Ground

Dir, USAMSAA  
ATTN: AMXSY-D  
AMXSY-MP, H. Cohen  
Cdr, USATECOM  
ATTN: AMSTE-TO-F  
Cdr, CRDC, AMCCOM  
ATTN: SMCCR-RSP-A  
SMCCR-MU  
SMCCR-SPS-IL